A Graphene-Quantum-Dot Ink-Printed Dual-Mode Bending Sensor for Biomedical Applications

Dilruba Alam, Azmin Islam, Peifen Zhu, Syed Kamrul Islam, and Mohammad Rafiqul Haider
Department of Electrical Engineering and Computer Science
University of Missouri
Columbia, MO, USA
{dilruba.alam, azmin.islam, pzhu, islams, mhaider}@missouri.edu

***Abstract*—The increasing demand for non-invasive, continuous, and user-friendly healthcare solutions is accelerating the development of advanced biomedical sensors. Flexible optoelectronic sensors, in particular, offer real-time, contactless physiological monitoring for applications such as smart health systems, remote diagnostics, and wearable devices. In this study, the fabrication and characterization of a dual-mode flexible bending sensor is presented that integrates graphene quantum dots with inkjet-printed silver interdigitated electrodes on a polyethylene terephthalate substrate. The sensor exhibits significant strain sensitivity, with the gauge factor increasing with decreasing bending diameter, demonstrating high responsiveness to mechanical deformation. Additionally, the photoluminescence emission peak shifts from 500 nm to 464 nm under strain, providing an optical strain-sensing mode. The sensor's stable dual-mode (electrical and optical) response across repeated bending cycles enhances its reliability and application versatility. This combined functionality makes the proposed sensor a promising candidate for wearable biomedical platforms that require real-time strain detection and contactless physiological monitoring.**

***Index Terms*—Graphene Quantum Dots, Inkjet-printing, Optoelectronic sensors, Photoluminescence, Flexible electronics.**

I. Introduction

Optoelectronic sensors integrate optical and electronic components to detect physiological signals and biomarkers in real time, typically in a non-invasive or minimally invasive manner. Flexible optoelectronic sensors, utilize materials such as quantum dots, organic semiconductors, perovskites, and nanostructured carbons like graphene and carbon nanotubes, and offer high sensitivity, mechanical durability, as well as multifunctionality under repeated bending or stretching. These sensors enable advanced devices, including photoplethysmography sensors, oximeters, and biosensors for fluid analysis and continuous health monitoring [1]–[5]. Flexible photodetectors and light-emitting diodes are also being developed for large-area, low-cost, and wearable systems with applications spanning biomedical sensing and photocommunication [5], [6]. Recent studies have shown that flexible optoelectronic sensors, especially those using colloidal quantum dots and graphene electrodes, maintain stable performance under cyclic mechanical stress, making them ideal for next-generation wearable monitors [7].

Modern flexible bending sensors employ various sensing mechanisms, including piezoresistive, photonic, magnetic, and triboelectric principles [8]. Piezoresistive sensors utilizing advanced materials such as microcracked gold nanofilms, porous graphene, carbon black composites, and silver nanowires have achieved superior sensitivity and long-term stability [9]. Photonic sensors using optical waveguides and Bragg gratings enable ultra-thin, highly flexible designs capable of detecting curvature, strain, and temperature simultaneously [10]. Recent innovations such as bianisotropic textiles now offer omnidirectional sensing (0–360°) with low error rates, making them effective for soft robotics and wearable joint monitoring [11].

Despite these advancements, significant gaps remain, particularly in interference resistance, multidirectional detection, and scalable, cost-effective fabrication. Many existing sensors rely on complex material processing or single-mode sensing, which limits their reliability and practical deployment.

Printed porous graphene and composite-based sensors have shown excellent durability, high linearity, and low hysteresis over extended cycles [12], [13], expanding their applications in wearable health monitoring, robotics, and interactive systems [13]–[15]. Unlike bulk graphene, graphene quantum dots (GQDs) exhibit a tunable bandgap influenced by their size, shape, and edge configuration [16]. They also provide strong size-dependent photoluminescence that stretches from ultraviolet to near-infrared, making them promising materials for biological imaging, optoelectronic devices, and sensors [17]. Electrically, GQD-based films exhibit tunneling-dominated conduction with high gauge factors (up to 841.42) and a wide range of deformation detection (up to 50%) [18], [19]. Optically, GQDs provide strain-tunable photoluminescence, allowing non-contact, real-time strain detection that is immune to electromagnetic interference [20], [21].

In this work, we propose a low-cost, flexible dual-mode strain sensor that integrates electrical and optical sensing using GQDs printed on a polyethylene terephthalate (PET) substrate. The proposed dual-sensing approach enhances reliability and versatility by enabling simultaneous detection of strain-induced resistance changes and photoluminescence (PL) variations.

The rest of the paper is organized as follows. Section II discusses the sensor's working mechanism. Section III outlines the fabrication process. The experimental results and analysis are presented in Section IV, followed by conclusions and future research directions in Section V.

II. Fundamentals of Strain Sensing in GQD Devices

A. Resistive Sensing via Quantum Electron Tunneling in Graphene Quantum Dots

GQDs are zero-dimensional sp^2 carbon nanostructures that exhibit tunable electronic and optical properties due to quantum confinement and edge effects [22]. In GQD-based thin films, one of the most significant charge transport mechanisms is quantum electron tunneling, where electrons can pass through a potential barrier that would be classically forbidden, particularly when the GQDs are separated by nanometer-scale dielectric gaps. The following equation describes the tunneling resistance between two adjacent nanomaterials based on Simmons' tunneling theory [23].

$$R_{\text{tunnel}} = \frac{V}{AJ} = \frac{h^2 d}{Ae^2\sqrt{2m\lambda}} \exp\left(\frac{4\pi d}{h}\sqrt{2m\lambda}\right) \tag{1}$$

where:

- V is the applied electrical potential difference,
- A is the cross-sectional area of the tunneling junction,
- J is the tunneling current density,
- h is Planck's constant,
- d is the distance between adjacent nanomaterials,
- e is the elementary charge,
- m is the mass of an electron,
- λ is the barrier height for tunneling.

As the distance d between increases, the tunneling resistance rises exponentially due to the reduced tunneling probability. This relationship is critical in flexible strain sensors where mechanical deformation changes the interparticle distance, modulating the sensor's resistance in response to strain, as shown in Fig. 1.

When mechanical strain ε is applied (e.g., through substrate bending), the average inter-dot distance increases, reducing the tunneling probability and thus increasing the film's resistance.

The relationship between the inter-dot distance and strain can be approximated by [24]:

$$d(\varepsilon) = d_0(1 + \alpha\varepsilon) \tag{2}$$

where d_0 is the initial distance and α is a geometric factor dependent on the material's deformation characteristics.

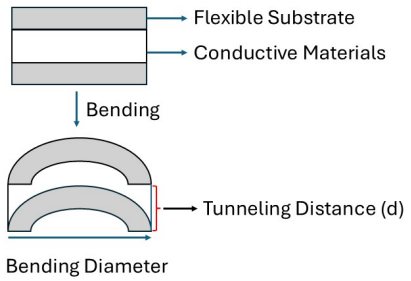

Fig. 1. Resistive sensing via quantum tunneling.

This tunneling-based resistive modulation is the fundamental sensing mechanism employed in the proposed dual-mode flexible strain sensor.

The strain sensitivity is typically quantified using the gauge factor:

$$\text{GF} = \frac{\Delta R/R_0}{\varepsilon} \tag{3}$$

B. Optical Sensing via Photoluminescence Modulation

GQDs show excitation-dependent photoluminescence because of their quantum-confinement and edge-functionalization properties. The optical properties are highly sensitive to size, shape, edge structure, and surface functionalization, and several peaks such as $s\ \sigma - \sigma^*$, $\pi - \pi^*$, $n - \pi^*$, and $n - \sigma^*$ can be observed in the photoluminescence (PL) spectra of the GQDs [25].

In the context of GQDs, when mechanical strain is applied, the wavelength shifts (red or blue) and intensity variations are observed in the emission spectra under different bending conditions, as demonstrated in Fig. 2. This enables the sensor to operate optically, without electrical connections, which is advantageous for bio-integrated or remote sensing platforms. The PL response changes due to:

- Quantum Confinement Alteration: Under tensile strain (e.g., outward bending), the sp^2 carbon domains in GQDs are spatially isolated, enhancing the confinement effects, increasing the energy gap, and resulting in a blue shift of PL spectra [26].
- Defect-State Perturbation: The bend modifies the functional groups of the surface and the oxygenated defects on the GQD surfaces, thereby changing the recombination pathways [27].

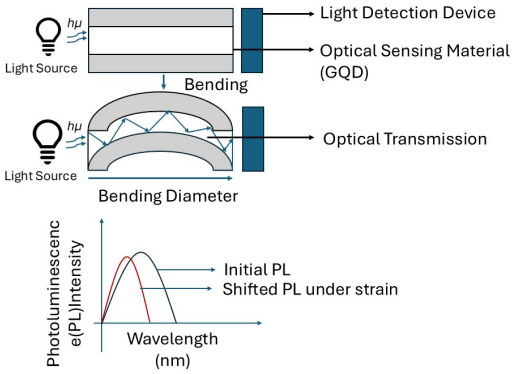

Fig. 2. Optical sensing mechanism of GQD based bending sensor

C. Working Principle of The Printed Bending Sensor

In the fabricated devices, electrons initially tunnel through nanogaps between GQDs, forming multiple conductive pathways in the unstrained state. When the PET substrate is bent, the inter-dot spacing increases, reducing the tunneling probability and disrupting the conductive network. Consequently, the number of active conduction paths (N) decreases, leading to a nonlinear increase in resistance that correlates with the

applied strain. Additionally, the quantum confinement effects and strain-induced modifications of surface states in GQDs result in photoluminescence shifts, enabling optical strain sensing. These underlying mechanisms support the use of GQD-based tunneling sensors for high-sensitivity, dual-mode (electrical and optical) strain detection.

These device physics models validate the choice of GQD-based tunneling sensors for high-strain, high-sensitivity, and dual-mode (electrical and optical) applications.

III. Sensor Fabrication and Characterization

A. Substrate and Electrode Fabrication

A flexible PET substrate, 250 μm thick, was cleaned using ethanol and deionized water. Silver nanoparticle ink was printed into an IDE structure using an inkjet printer. The printed pattern consisted of 5 fingers per side, each with a width of 1 mm and spacing of 0.5 mm. The ink was cured at 80°C for 30 minutes.

B. GQD Deposition

GQDs used in this study were obtained as received from Sigma-Aldrich without further modification. The GQD solution was diluted to 1 mg/mL and drop-cast onto the IDE region to form a thin film bridging the electrodes. The substrate was subsequently dried at 80°C to ensure proper film formation as shown in Fig. 3.

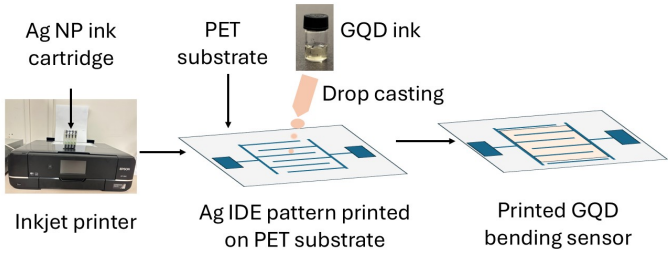

Fig. 3. Schematic illustration of the fabrication process of the printed GQD bending sensor. Silver nanoparticle (Ag NP) ink is patterned as IDEs on a PET substrate using inkjet printing. GQD ink is subsequently drop-cast onto the printed electrodes to complete the sensor structure.

C. Strain Application and Testing

Mechanical strain was applied by bending the PET substrate over cylindrical surfaces of known radii. Electrical measurements were conducted using a Keithley 2400 Source Meter, and current-voltage (I-V) curves were recorded for each bending configuration. Optical characterization was performed using the Fluorescence Spectrometer to capture emission spectra as demonstrated in Fig. 4

IV. Results and Discussion

A. Electrical Measurements

The electrical performance of the fabricated flexible sensor was evaluated through current–voltage (I–V) measurements under different bending conditions: no bending, 2 cm diameter bending, 1 cm diameter bending, and 0.5 cm diameter bending. For the unstrained condition, the sensor exhibited a linear response with a maximum current of approximately ±800nA, as observed in Fig. 5. As strain was increased by reducing the bending radius, the current decreased significantly, indicating a sharp rise in resistance due to reduced tunneling probability. I-V curves revealed nonlinear characteristics, with current decreasing under higher strain. The resistance increased with tighter bending radii, supporting the tunneling-based model. The gauge factor (GF) of the fabricated dual-mode strain sensor was analyzed for bending diameters of 2 cm, 1 cm, and 0.5 cm. The results showed a clear quantitative trend where the GF increased as the bending radius decreased, indicating higher strain sensitivity under tighter bending conditions. Specifically, the sensor exhibited a relatively lower GF at 2 cm bending compared to significantly higher values at 1 cm and 0.5 cm.

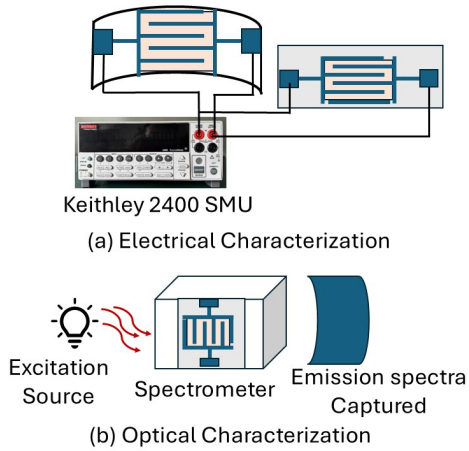

Fig. 4. Schematics of the characterization methods used for the printed GQD bending sensor. (a) Electrical characterization setup using a source meter to measure resistance changes under different bending conditions. (b) Optical characterization setup where the sensor is excited by a light source, and the resulting photoluminescence emission spectra are captured using a spectrometer.

The voltage sweep from –10 V to +10 V confirmed a symmetric response, indicating good stability and no significant hysteresis during bending and unbending cycles. Overall, these results demonstrate that the sensor can reliably detect bending-induced strain by monitoring changes in electrical current.

B. Photoluminescence Analysis

Although the GQD samples exhibited photoluminescence responses under various excitation wavelengths, including 275 nm, 325 nm, 350 nm, and 380 nm, the excitation at 250 nm consistently produced the strongest, most stable, and quantifiable photoluminescence signal across repeated measurements. Under 250 nm excitation, the unstrained GQD film exhibited a sharp and high-intensity emission peak at 500 nm. Upon bending, the emission peak shifted to 464 nm with a significant reduction in intensity and noticeable broadening as shown in Fig. 6. This blue-shift and spectral broadening are attributed to

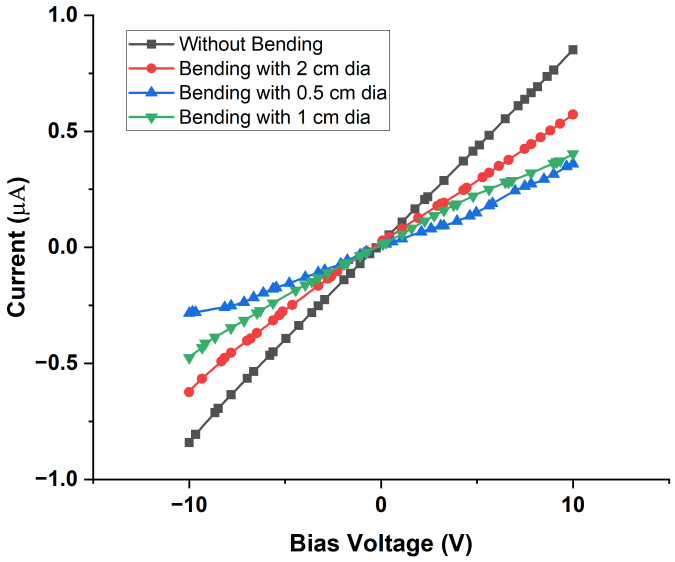

Fig. 5. I-V curve of the sensor showing gradual decrease in slope with continuous increase in strain due to bending.

strain-induced changes in quantum confinement and inter-dot electronic coupling. This mechanism agrees with the trends observed in our data: a PL peak shift from 500 nm (unbent) to 464 nm (bent), consistent with reports that show strain-induced blue-shifting due to enhanced confinement effects in quantum-confined systems [28], [29].

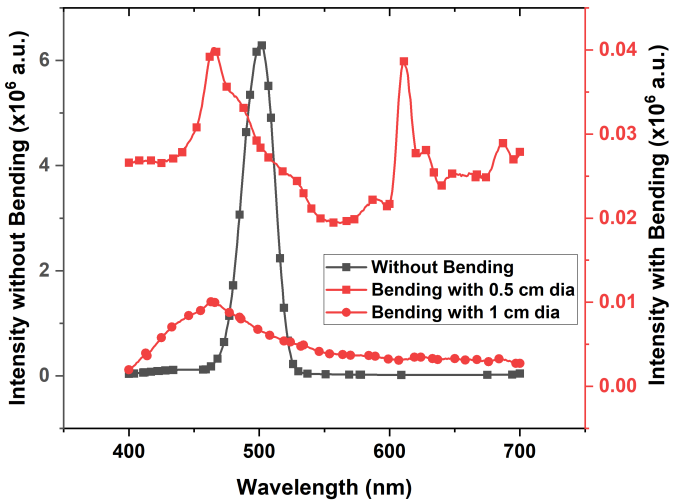

Fig. 6. Bending effects on emission spectra with 250 nm excitation.

These results align with reports in the literature. For instance, strain-induced photoluminescence modulation has been demonstrated in flexible heterostructures [27], and studies on biaxial strain application reveal reversible shifts in PL emission due to modulated energy band profiles [28]. Additionally, spatial/spectral isolation of emitters through strain gradients has been shown in 2D materials [29].

Under 365 nm excitation, the unstrained GQD film emitted at 470 nm. Upon bending, the emission peak red-shifted to 490 nm, with a slight reduction in intensity. A similar trend was observed for 450 nm excitation, though with less shift. This confirms the PL modulation with strain, aligning with reports on GQD band structure sensitivity [26], [30].

C. Synergistic Dual-Sensing Behavior

The hybrid electrical-optical mechanism enables strain detection through both tunneling resistance modulation and photoluminescence spectral shifts. The electrical mode provides real-time response and seamless integration with electronic circuits, while the optical mode offers contactless readout with the potential for imaging strain distribution. Together, these synergistic responses enhance the reliability, redundancy, and versatility of the sensor for a wide range of applications.

V. Conclusion

A dual-mode flexible strain sensor utilizing GQDs on inkjet-printed silver IDEs over a PET substrate has been demonstrated. The sensor exhibited reliable electrical and optical responses under varying bending conditions. Electrical measurements confirmed a notable decrease in current with increased strain, corresponding to a higher GF. Photoluminescence analysis revealed a blue shift from of 36nm and considerable intensity reduction under strain, validating strain-tunable photoluminescence. These results confirm the sensor's ability to detect strain through both resistive and optical modes, providing redundancy and improved reliability. The proposed sensor is particularly promising for wearable biomedical applications, including monitoring of human motion, tissue swelling, and subtle mechanical changes such as cellular traction forces. The optical sensing capability further enables non-contact, real-time strain visualization, which could support cancer mechanobiology studies, and nanoparticle–biosystem interaction tracking in future flexible biomedical platforms.

Acknowledgment

This work was supported by the USA National Science Foundation (NSF) under Grant No. ECCS-2430440. Any opinions, findings, conclusions, or recommendations expressed in this material are those of the author(s) and do not necessarily reflect the views of the National Science Foundation.

References

[1] Ahmed, M., Ting, J., Arias, A., Nagisetty, R., Khan, Y., & Han, D. (2019). Organic Multi-Channel Optoelectronic Sensors for Wearable Health Monitoring. IEEE Access, 7, 128114-128124. https://doi.org/10.1109/ACCESS.2019.2939798.

[2] Alam, M., Imran, M., & Shariq, M. (2021). Optoelectronics for Biomedical Applications. Nanomaterials for Optoelectronic Applications. https://doi.org/10.1201/9781003083948-8.

[3] M. R. Opu, S. D. Gardner and M. R. Haider, "A Low-Cost Inkjet-Printed Heart Sound Sensor for Telehealth Application," 2023 IEEE 66th International Midwest Symposium on Circuits and Systems (MWSCAS), Tempe, AZ, USA, 2023, pp. 197-201, doi: 10.1109/MWSCAS57524.2023.10405897.

[4] R. Lu, M. R. Haider, S. Gardner, J. I. D. Alexander, and Y. Massoud, "A paper-based inkjet-printed graphene sensor for breathing-flow monitoring," *IEEE Sensors Letters*, vol. 3, no. 2, pp. 1–4, 2018.

[5] Choi, M., Yoo, J., Chang, S., Kim, D., Kim, M., Koo, J., & Song, Y. (2024). Flexible and Stretchable Light-Emitting Diodes and Photodetectors for Human-Centric Optoelectronics.. Chemical reviews. https://doi.org/10.1021/acs.chemrev.3c00548.

[6] Deng, W., Xie, M., Xiong, D., Yan, W., Yang, W., Huang, H., Jin, L., Jin, H., Chun, F., Deng, W., Luo, C., Zhang, H., Chu, X., Li, W., & Liu, C. (2019). All-Sprayed-Processable, Large-Area, and Flexible Perovskite/MXene-Based Photodetector Arrays for Photocommunication. Advanced Optical Materials, 7. https://doi.org/10.1002/adom.201801521.

[7] Yang, J., Shin, K., Kim, S., Choi, M., Park, S., Hur, J., Hwang, S., Lee, C., Kim, T., Hyeon, T., Yoon, Y., Lee, S., & Kim, D. (2017). Fully Stretchable Optoelectronic Sensors Based on Colloidal Quantum Dots for Sensing Photoplethysmographic Signals.. ACS nano, 11 6, 5992-6003 . https://doi.org/10.1021/acsnano.7b01894.

[8] Peng, Y., Li, S., Xia, Z., Chen, X., Zhang, F., Zhong, L., Liu, W. (2024). Recent advances in flexible bending sensors and their applications. International Journal of Smart and Nano Materials, 15(4), 697–729. https://doi.org/10.1080/19475411.2024.2417834.

[9] Liao, X., Zhang, Z., Liao, Q., Liang, Q., & Zhang, Y. (2017). Flexible, Cuttable, and Self-Waterproof Bending Strain Sensors Using Microcracked Gold Nanofilms@Paper Substrate.. ACS applied materials & interfaces, 9 4, 4151-4158. https://doi.org/10.1021/acsami.6b12991.

[10] Annunziato, A., Prudenzano, F., Dulieu-Barton, J., Anelli, F., Holmes, C., & Godfrey, M. (2024). Flexible Photonic Sensors: Investigation of an Approach Based on Ratiometric Power in Few-Mode Waveguides for Bending Measurement. IEEE Access, 12, 29166-29174. https://doi.org/10.1109/ACCESS.2024.3368885.

[11] Jin, C., Jiang, M., & Bai, Z. (2024). Omnidirectional Bending Sensor with Bianisotropic Structure for Wearable Electronics.. ACS sensors. https://doi.org/10.1021/acssensors.4c02734.

[12] Xu, Z., Song, X., Yang, Q., Zhang, M., Pang, K., & Peng, Y. (2020). A Flexible and Stretchable Bending Sensor Based on Hydrazine-Reduced Porous Graphene for Human Motion Monitoring. IEEE Sensors Journal, 20, 12661-12670. https://doi.org/10.1109/JSEN.2020.3002916.

[13] Tokito, S., Takeda, Y., Yoshida, A., Sekine, T., Wang, Y., & Kumaki, D. (2023). Printed Directional Bending Sensor with High Sensitivity and Low Hysteresis for Human Motion Detection and Soft Robotic Perception. Sensors (Basel, Switzerland), 23. https://doi.org/10.3390/s23115041.

[14] Fan, B., Wu, B., Li, M., Guo, X., & Chen, S. (2020). Printed Flexible Strain Sensor Array for Bendable Interactive Surface. Advanced Functional Materials, 30. https://doi.org/10.1002/adfm.202003214.

[15] Kim, M., Kim, K., Kim, T., Park, I., Jeong, Y., Kwon, D., Lee, T., Amjadi, M., Kim, S., & Oh, Y. (2019). Wearable, Ultrawide-Range, and Bending-Insensitive Pressure Sensor based on Carbon Nanotube Network-Coated Porous Elastomer Sponges for Human Interface and Healthcare Devices.. ACS applied materials & interfaces. https://doi.org/10.1021/acsami.9b07636.

[16] Voznyy, O., Güçlü, A., Korkusiński, M., Kadantsev, E., Potasz, P., Sheng, W., Zieliński, M., & Hawrylak, P. (2011). Electronic and optical properties of semiconductor and graphene quantum dots. Frontiers of Physics, 7, 328 - 352. https://doi.org/10.1007/s11467-011-0200-5.

[17] Tang, L., Teng, K., Lau, S., & Tian, P. (2018). Graphene quantum dots from chemistry to applications. Materials Today Chemistry. https://doi.org/10.1016/J.MTCHEM.2018.09.007.

[18] Huina Zhang, Zhongyun Yuan, Kai Zhuo, Qiang Zhang, Wendong Zhang, Lihua Liu, S. Sang, Jianlong Ji and Dong Zhao. "Performance of CNTs/GQD-Based Flexible Strain Sensors.." Journal of nanoscience and nanotechnology, 20 2 (2020): 1013-1019 . https://doi.org/10.1166/jnn.2020.16905.

[19] Jisheng Han, Dechao Chen, Shujun Wang, P. Tanner, M. Lobino, F. Lenzini, Qin Li and David Thiel. "Chemically derived graphene quantum dots for high-strain sensing." Journal of Materials Science & Technology (2022). https://doi.org/10.1016/j.jmst.2022.08.041.

[20] Abramson A, Chan CT, Khan Y, Mermin-Bunnell A, Matsuhisa N, Fong R, Shad R, Hiesinger W, Mallick P, Gambhir SS, Bao Z. A flexible electronic strain sensor for the real-time monitoring of tumor regression. Sci Adv. 2022 Sep 16;8(37):eabn6550. doi: 10.1126/sciadv.abn6550. Epub 2022 Sep 16. PMID: 36112679; PMCID: PMC9481124.

[21] P. P. Pancham, W.-H. Chiu, A. Mukherjee, C.-Y. Lo, Strain Visualization in Flexible Sensors with Functional Materials: A Review. Adv. Mater. Interfaces 2023, 10, 2300029. https://doi.org/10.1002/admi.202300029

[22] T. S. Sreeprasad, A. A. Rodriguez, J. Colston, S. Graham, and V. Berry, "Electron-tunneling modulation in percolating network of graphene quantum dots: Fabrication, phenomenological understanding, and humidity/pressure sensing applications," *Nano Letters*, vol. 13, no. 4, pp. 1757–1763, 2013.

[23] Amjadi, M., Kyung, K.-U., Park, I. and Sitti, M. (2016), Stretchable, Skin-Mountable, and Wearable Strain Sensors and Their Potential Applications: A Review. Adv. Funct. Mater., 26: 1678-1698. https://doi.org/10.1002/adfm.201504755

[24] J. Zhao et al., "Tunable piezoresistivity of nanographene films for strain sensing," *ACS Nano*, vol. 9, no. 2, pp. 1622–1629, 2015.

[25] H. Cho, G.Bae, and B.H. Hong, "Engineering functionalization and properties of graphene quantum dots (GQDs) with controllable synthesis for energy and display applications," *Nanoscale*, vol. 16, no. 7, pp. 3347–3378, Jan. 2024, doi:10.1039/D3NR05842E.

[26] Z. Zhou et al., "Flexible optical strain sensors based on photoluminescent carbon nanomaterials," *Advanced Optical Materials*, vol. 9, no. 11, 2021.

[27] Y. Zhang et al., "Mechanically Controlled Reversible Photoluminescence in Flexible Transparent Heterostructures," *ACS Applied Materials & Interfaces*, vol. 12, no. 32, pp. 36217–36225, 2020.

[28] H. Liu et al., "Biaxial strain modulation of photoluminescence in two-dimensional materials," *Nano Energy*, vol. 117, p. 108551, 2024.

[29] A. Branny et al., "Deterministic strain-induced arrays of quantum emitters in a two-dimensional semiconductor," *Nature Communications*, vol. 8, no. 1, p. 15053, 2017.

[30] Y. Liu et al., "Strain-tunable photoluminescence in graphene quantum dots: Mechanisms and applications," *ACS Nano*, vol. 13, no. 5, pp. 5630–5640, 2019.